Published for SISSA by Springer

Received: *May 4, 2018*
Accepted: *July 29, 2018*
Published: *September 10, 2018*

S-matrix bootstrap for resonances

N. Doroud and J. Elias Miró

SISSA/ISAS and INFN,
Via Bonomea, 265 Trieste, Italy

E-mail: ndoroud@sissa.it, jelias@sissa.it

Abstract: We study the $2 \to 2$ S-matrix element of a generic, gapped and Lorentz invariant QFT in $d = 1+1$ space time dimensions. We derive an analytical bound on the coupling of the asymptotic states to unstable particles (a.k.a. resonances) and its physical implications. This is achieved by exploiting the connection between the S-matrix phase-shift and the roots of the S-matrix in the physical sheet. We also develop a numerical framework to recover the analytical bound as a solution to a numerical optimization problem. This later approach can be generalized to $d = 3 + 1$ spacetime dimensions.

Keywords: Field Theories in Lower Dimensions, Nonperturbative Effects, Integrable Field Theories

ArXiv ePrint: 1804.04376

https://doi.org/10.1007/JHEP09(2018)052

Contents

JHEP09(2018)052

1 Introduction

Deriving the phenomenological implications of strongly coupled Quantum Field Theories (QFT) is hard. Any new idea or approach to inspect such strongly coupled regime deserves to be scrutinized. The recent progress on the numerical conformal bootstrap [1–5] — reviving the successful $d = 1 + 1$ conformal bootstrap [6, 7] — has lead to a revision of the closely related S-matrix bootstrap [8, 11].

The old analytical S-matrix bootstrap approach lost momentum with the advent of QCD and due to the difficulties of dealing with the analytic properties of the S-matrix in $d = 3 + 1$ spacetime dimensions.[1] For a compendium of results on the analytic properties of the S-matrix see for instance [13]. In the present context *bootstrap* is synonymous to an axiomatic approach, where out of few physical assumptions one extracts general consequences for physical observables. For the S-matrix bootstrap approach, the input assumptions are those of quantum mechanics, special relativity and assumptions on the spectrum of particles encoded through analytic properties of the S-matrix elements.

Lately, there has been a number of interesting results within the S-matrix bootstrap approach [8–10]. The key aspects that paved the way for these developments have been to, firstly, identify an interesting and simple enough question that the bootstrap approach can answer and, secondly, the development of a numerical approach to answer the question in general spacetime dimensions. Specifically, ref. [9] found a rigorous analytical upper bound on the coupling between asymptotic states of the S-matrix in $d = 1 + 1$ dimensions. The existence of such upper bound was expected in higher dimensions and was demonstrated in $d = 3 + 1$ by means of a numerical approach ref. [10].

Exploring the space of consistent S-matrices in $d = 3 + 1$ has lots of potential applications for particle physics. For a realistic set up though we would like to study S-matrices that feature unstable resonances. The main purpose of this work is to take the first steps towards developing this theory. The present work is entirely in $d = 1 + 1$ and we focus on the $2 \to 2$ S-matrix element of the single stable particle of the theory. These simplifying assumptions will allow us to derive a number of analytical results and intuition that is important before attacking the analogous problem in $d = 3 + 1$.

Section 2 is mostly review and discussion of the analytic properties of the S-matrix. Section 3 contains the main result, a bound on the $2 \to 2$ S-matrix elements that feature unstable resonances. We discuss the interpretation of this bound and the implications for the spectrum of resonances. In section 4 we perform a numerical study that matches the analytical derivations of section 3. Crucially, the numerical approach presented in section 4 admits a generalization to $d = 3 + 1$ dimensions. Finally, we conclude and outline possible directions to develop.

2 Analytic properties of the S-matrix

The main focus of this paper is to study the space of consistent S-matrices in $d = 1 + 1$ spacetime dimensions. For simplicity we restrict our attention to theories with only a single

[1] See ref. [12] for a testimony.

JHEP09(2018)052

stable particle of mass m. This is not crucial and the assumption can be relaxed on later studies. We focus on the elastic $2 \to 2$ S-matrix element

$$\langle p_1, p_2|\hat{S}|p_3, p_4\rangle \equiv \mathbb{1}\, S(p_i)\,, \tag{2.1}$$

where $\mathbb{1} = \langle p_1, p_2|p_3, p_4\rangle$ captures the kinematical information. All the interesting physics is encoded in the Lorentz scalar S which is a function of the Mandelstam variable $s = (p_1 + p_2)^2$. Note that in two spacetime dimensions the scattering is along a line and thus there is no scattering angle. Consequently either of the Mandelstam variables $t = (p_1 + p_3)^2$ or $u = (p_1 + p_4)^2$ must vanish, which together with the kinematical constraint $s+t+u = 4m^2$, imply that the function S in eq. (2.1) is only a function of a single variable s. This function is further constrained by crossing symmetry

$$S(s) = S(4m^2 - s)\,, \tag{2.2}$$

i.e. it is symmetric under the exchange of the s and t channels (or equivalently between the s and u channels). In the rest of this section we will review the analytic properties of $S(s)$.

Consider the analytical continuation of $S(s)$ into the complex s-plane. Generically the function $S(s)$ has branch point singularities at the minimal values of s where the process $2 \to n$ is kinematically allowed. For positive s, the lowest such branch point is at $s = (2m)^2$, the two-particle branch point. Crossing symmetry (2.2) implies the presence of a corresponding branch point at $s = 0$. Generically, in the absence of extra symmetries forbidding particle production, infinitely many branch points are expected on the real line at the minimal values where higher-particle production is kinematically allowed. We have illustrated the branch points at $s = 4m^2, 9m^2$ (red circles) and the crossing related $s = 0, -5m^2$ (red squares) in the left plot of figure 1. The physical S-matrix is obtained in the limit

$$\lim_{\epsilon \to 0^+} S(s + i\epsilon)\,, \tag{2.3}$$

namely by approaching the real line from above without encircling any such branch points. The physical s-plane is defined as the trivial analytical continuation of eq. (2.3) without encircling any branch point. Pictorially, it consists of the full complex plane minus the cuts on the real axis, see figure 1. The two key analytical assumptions on $S(s)$ are that all the singularities of the physical s-plane consist only of branch points on the real line;[2] and that along the real axis and below the two-particle threshold $S(s)$ is a real function. Thus the analytic continuation of $S(s)$ satisfies

$$S^*(s) = S(s^*)\,, \tag{2.4}$$

which is often referred to as *real analyticity*.[3]

[2] We assume a Z_2 symmetry forbidding a cubic self-interaction of the stable particle. Such cubic self-interaction would lead to poles at $s = m^2, 3m^2$.

[3] Let us note that in eq. (2.4) we have assumed that the S-matrix theory is invariant under space parity. The general condition for the two-body S-matrix is Hermitian analyticity $S^*_{ij}(s) = S_{ji}(s^*)$ which reduces to real analyticity only for parity invariant theories [14].

JHEP09(2018)052

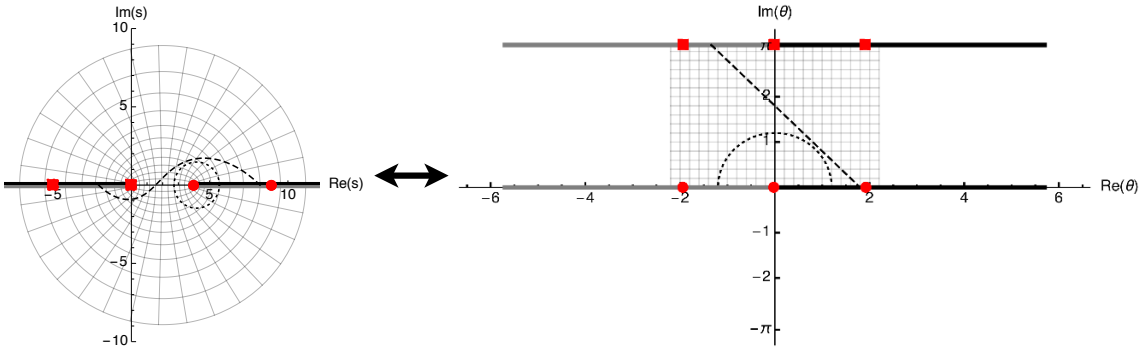

Figure 1. Illustration of the conformal map in eq. (2.8). The complex s-plane, the left plot, is mapped into the complex θ-strip $\mathrm{Im}\,\theta \in (0, \pi)$, right plot. We have also depicted the mapping of a dashed curve, a dotted curve and a gray grid.

The last property of $S(s)$ follows from unitarity of the full S-matrix, implying the following constraint on the $2 \to 2$ S-matrix element

$$S(s + i\epsilon)S(s - i\epsilon) = f(s) \qquad \text{with} \quad 0 \leqslant f(s) \leqslant 1\,, \tag{2.5}$$

and $s > 4m^2$. Note that we have used real analyticity to write the modulus as $|S(s+i\epsilon)|^2 = S(s + i\epsilon)S(s - i\epsilon)$. Recall that below the inelastic threshold s_* (above which $2 \to n$, with $n > 2$, processes are kinematically allowed) and above the two-particle production threshold, unitarity is saturated

$$f(s) = 1 \qquad \text{for} \quad 4m^2 < s \leqslant s_*\,. \tag{2.6}$$

Typically the inelastic threshold is at the three-particle production threshold $s_* = 9m^2$ or four-particle production threshold $s_* = 16m^2$.

Unless explicitly stated otherwise, we will refer to $S(s)$ as the *S-matrix* (instead of *the $2 \to 2$ S-matrix element function*). To summarize, the S-matrix is assumed to satisfy crossing (2.2), real-analyticity (2.4), unitarity (2.5) and there are no singularities in the physical s-plane but only branch points on the real line associated with the $2 \to n$ ($n \geqslant 2$) scattering processes. In order to further elucidate the analytical properties of the S-matrix we will next review a particularly simple S-matrix. This will also serve as an excuse to introduce the rapidity variable θ which we will use in the rest of the paper.

2.1 The θ-strip

Consider the following classic QFT example in $d = 1{+}1$: the Sine-Gordon S-matrix element for the scattering of the lightest breather is given by [15, 16]

$$S_{\mathrm{SG}}(s) = \frac{\sqrt{s}\sqrt{4m^2 - s} + m_1\sqrt{4m^2 - m_1^2}}{\sqrt{s}\sqrt{4m^2 - s} - m_1\sqrt{4m^2 - m_1^2}}\,, \tag{2.7}$$

where s is the Mandelstam variable. The function $S_{\mathrm{SG}}(s)$ has a pole at $s = m_1^2$, the mass of the next-to-lightest breather. The matrix element $S_{\mathrm{SG}}(s)$ has branch points at $s = 0,\ 4m^2$

JHEP09(2018)052

associated with the two-particle production threshold. These are square-root branch points and can be resolved by the conformal map

$$s(\theta) = 4m^2 \cosh^2(\theta/2)\,. \tag{2.8}$$

Eq. (2.8) maps the entire physical s-plane minus the cuts on the real line into the strip

$$\mathrm{Im}\,\theta \in (0, \pi)\,, \tag{2.9}$$

which we will refer to as the *physical strip*. The transformation is illustrated in figure 1. The two-to-two S-matrix element (2.7) in the θ-strip is given by

$$S_{\rm SG}(\theta) \equiv S_\alpha = \frac{\sinh\theta - \sinh\alpha}{\sinh\theta + \sinh\alpha}\,, \tag{2.10}$$

where $\sinh\alpha = -i\,m_1/m\sqrt{1-m_1^2/(4m^2)}$, and we defined $S_\alpha(\theta)$ for later use.[4] Eq. (2.10) is analytic at the points $\theta = 0$ and $\theta = i\pi$, corresponding to the original branch points of eq. (2.7) at $s = 4m^2$ and $s = 0$ respectively. The second Riemann sheet of (2.7) reached by traversing a branch cut stemming from the two-particle branch points at $s = 0, 4m^2$ is mapped into $\mathrm{Im}\,\theta \in (-\pi, 0)$. Note also that the lines $\theta = -i\pi$ and $\theta = i\pi$ are identified; $\mathrm{Im}\,\theta \in [-\pi, \pi)$ is the fundamental domain of eq. (2.10), which is periodic under $\theta \sim \theta + 2\pi i$.

The Sine-Gordon theory is very special as it is an integrable QFT. It follows that there is no particle production and the full S-matrix factorizes into the product of $2 \to 2$ matrix elements. Consequently $S_{\rm SG}(\theta)$ is a meromorphic — and thus single valued — function in the θ-strip $\mathrm{Im}\,\theta \in [-\pi, \pi)$. For a generic non-integrable QFT however, one has branch points at the inelastic thresholds $s = \{(3m)^2, (4m)^2, \ldots\}$ where the matrix elements $S_{2\to 3,4\ldots}$ are switched on. Those are mapped into the real line of the θ-strip. As depicted in figure 1, they appear both in the positive and negative real axis of the θ-strip because they can be reached from both Riemann sheets associated to the two-particle branch point.

As we have seen, the branch point at the two-particle production threshold in the particular example eq. (2.7) is two-sheeted. It turns out that this feature is more general and extends to non-integrable S-matrices, see appendix A for further details. The results of this paper however do not make use of the nature of any of the branch points in the physical s-plane.

In $d = 1{+}1$ dimensions θ has the physical interpretation of being the rapidity difference of the incoming particles $\theta \equiv \theta_2 - \theta_1$ where $p_i = (m\cosh\theta_i,\, m\sinh\theta_i)$. The S-matrix literature in $d = 1 + 1$ dimensions commonly uses this variable. Thus, in the rest of the paper we will consider the S-matrix as a function $S(\theta)$ (this is however not crucial and all the results below can be reformulated in the s-plane). For completeness, let us recall that crossing symmetry (2.2) in the θ-strip implies

$$S(\theta) = S(i\pi - \theta)\,, \tag{2.11}$$

real analyticity (2.4) reads

$$S^*(\theta) = S(-\theta^*)\,, \tag{2.12}$$

[4]The function $S_\alpha(\theta)$ is commonly called a Coleman-Dalitz-Dyson (CDD) factor.

JHEP09(2018)052

and unitarity (2.5) in the θ-strip reads

$$S(\theta)S(-\theta) = f(\theta)\,, \tag{2.13}$$

where $0 \leqslant f(\theta) \leqslant 1$ for real θ.

3 Unstable resonances

Our goal is to study QFTs with unstable particles or resonances. In this section, we first present the operational definition of a resonance before deriving a bound for the S-matrices that feature resonances. Finally, we discuss the interpretation of the bound in the context of a weakly coupled QFT.

3.1 What are unstable resonances?

In perturbation theory unstable particles are often associated with complex poles. These poles lie on higher Riemann sheets that can be reached by traversing the multi-particle branch cuts along the real line in the θ-plane.[5] The distinguishing feature of such singularities is that they lead to pronounced variations of the phase of the S-matrix evaluated along the real line. Thus, we define a resonance as an abrupt change in the phase of the S-matrix

$$\mathrm{Re}\, 2\delta(\theta) \qquad \text{where} \quad 2i\delta(\theta) \equiv \log S(\theta)\,, \tag{3.1}$$

without any reference to poles in higher Riemann sheets.

Abrupt variations of the phase of the S-matrix typically signal the presence of poles or zeros of the S-matrix in the complex plane and it is up to us to classify such pronounced features of the S-matrix. Of particular interest is when the phase of $S(\theta)$ abruptly increases by 2π continuously and monotonically in θ. Such 2π phase-shifts stem from the presence of a pair of zeros in the S-matrix $S(\theta)$ in the physical strip $\mathrm{Im}\,\theta \in (0, \pi)$. In fact, each zero in the physical θ strip contributes with an $i\pi$ to the total S-matrix phase shift[6]

$$2\int_{-\infty}^{\infty} d\theta\, \partial_\theta \delta(\theta) = \sum_{\text{zeros}} \pi\,. \tag{3.2}$$

Due to crossing symmetry, the zeros θ_i of $S(\theta)$ come in pairs related by crossing $S(\theta_i) = S(i\pi - \theta_i) = 0$. In addition, by real analyticity, the roots are also pairwise related by complex conjugation $S^*(\theta_i) = S(-\theta_i^*) = 0$. In many physically relevant S-matrices one finds an approximate 2π change of the phase in a bounded span $\theta \in [\theta_\circ - \gamma, \theta_\circ + \gamma]$

$$2\Delta\delta \equiv 2\int_{\theta_\circ-\gamma}^{\theta_\circ+\gamma} \partial_\theta \delta(\theta)\, d\theta \approx 2\pi\,, \tag{3.3}$$

where $\theta_\circ = \mathrm{Re}\,\theta_i$ and $\gamma \sim 2\,\mathrm{Im}\,\theta_i$, the exact choice of the resonance region $\theta_\circ \pm \gamma$ is somewhat arbitrary. This is the kind of resonances that we are interested in this paper.

[5] See appendix C.2 for an explicit example.

[6] See appendix B for the derivation of eq. (3.2) — this is the relativistic analog of Levinson's theorem, see for instance chapter XVII of [17].

JHEP09(2018)052

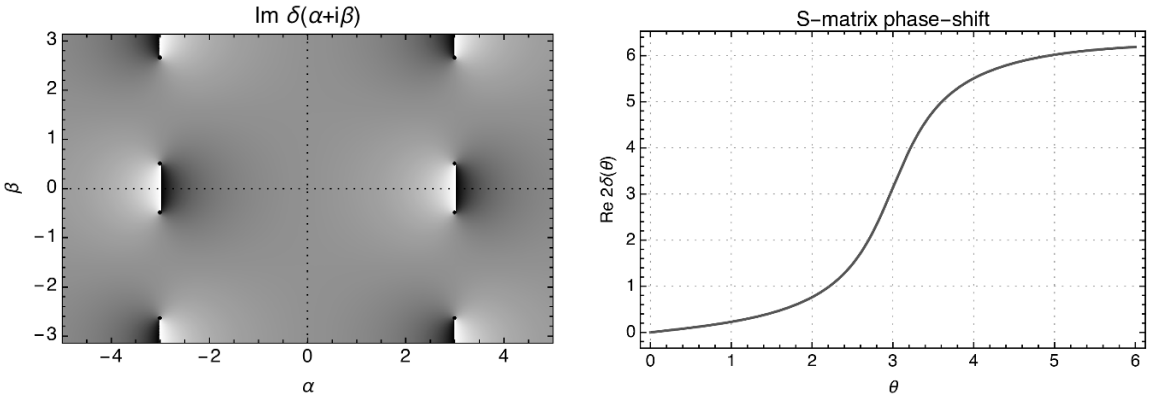

Figure 2. *Left*: section of the complex plane of the phase of eq. (3.5), the lines $\delta(i\pi) \sim \delta(-i\pi)$ should be indentified. *Right*: phase-shift of eq. (3.5) localized around the position of the branch points generated by the zeros and poles of $S_{\rm ex}(\theta)$.

3.1.1 Further comments

For a long-lived unstable particle associated to a long time delay, the 2π phase-shift is highly localized and $\mathrm{Im}\,\theta_i \ll 1$. The zeros in the physical strip are accompanied by poles which are hidden behind the multi-particle branch cuts. In terms of the θ variable the S-matrix behaves as

$$e^{2i\delta(\theta)} \sim e^{2i\delta_0}\,\frac{\theta-\theta_i}{\theta-\theta_i^*}\,, \tag{3.4}$$

for θ close to $|\theta_i|$. The zeros and poles of $S(\theta)$ result in branch points of $\delta(\theta)$. Pictorially, this leads to a branch cut that "cuts" the real line. Then, when evaluating $2\delta(\theta)$ along the real line the 2π phase-shift is a consequence of changing Riemann sheet of the logarithm.

As an illustration, consider the following function

$$S_{\rm ex}(\theta) = S_\alpha(\theta) S_{-\alpha^*}(\theta)\,, \tag{3.5}$$

where $\mathrm{Im}\,\alpha > 0$ and $S_\alpha(\theta)$ was defined in eq. (2.10). The function $S_{\rm ex}(\theta)$ is a realistic S-matrix element because it satisfies the unitary equation, crossing symmetry and it is real analytic.[7] $S_{\rm ex}(\theta)$ has zeros at $\theta = \alpha, -\alpha^*$ and poles at complex conjugate points as required by unitarity $S_{\rm ex}(\theta)S_{\rm ex}(-\theta) = 1$. The left plot in figure 2 shows a section of the fundamental domain of the complex plane of $\mathrm{Im}\,\delta(\theta)$ that includes the zeros and poles of $S(\theta)$. We have depicted branch cuts connecting the zeros on the physical strip with the poles on the lower stip $\theta \in (-\pi, 0)$. The branch cuts intersect the real line along which the physical S-matrix is evaluated. On the right hand side we have ploted $\mathrm{Re}\,2\delta(\theta)$ on a segment along the real line. As $2\delta(\theta)$ goes through the region $\theta \approx \mathrm{Re}\,\alpha$, i.e. near the location of the branch points, the function $2i\delta = \log S$ is evaluated in a higher Riemann sheet and the imaginary part is shifted by 2π. In section 3.3 we discuss a perturbative QFT with the same qualitative picture as the S-matrix in eq. (3.5).

[7] Note however that a generic product of CDD factors leads to a finite volume spectrum $E_i(R)$ with branch point singularities at finite volume [18, 19].

JHEP09(2018)052

To close up this section, let us insist that in general we will not refer to complex poles of the S-matrix. Instead, we focus on the zeros of $S(\theta)$ in the physical θ-strip (or physical s-plane), which are in a one-to-one correspondence with each π contribution to the total phase-shift (3.2). This picture avoids the need to discuss the nature of the branch points of $S(\theta)$ on the real line and the analytical continuation of the function $S(\theta)$ around such branch points which requires a case by case analysis. Instead, it only requires the trivial analytical continuation of $S(\theta)$ into the physical sheet which, by definition, is always available. Note also that the operational definition of unstable resonance that we are employing is physically meaningful because the phase-shift is experimentally accessible (it can also be extracted from lattice Monte Carlo simulations [20]).

3.2 A bound on the S-matrix of unstable resonances

The two-dimensional S-matrix can be written as follows

$$S(\theta) = \prod_j S_{\alpha_j}(\theta) \exp\left(- \int_{-\infty}^{+\infty} \frac{d\theta'}{2\pi i} \frac{\log f(\theta')}{\sinh(\theta - \theta' + i\epsilon)} \right) \qquad \text{for} \quad \text{Im}(\theta) \in [0, \pi) \tag{3.6}$$

where ϵ is an arbitrarily small positive parameter and $S_{\alpha_j}(\theta)$ denotes a CDD factor defined in (2.10):

$$S_\alpha(\theta) = \frac{\sinh\theta - \sinh\alpha}{\sinh\theta + \sinh\alpha} \,.$$

The set $\{\alpha_j\}$ parametrizes the position of the zeros and poles of $S(\theta)$ in the physical strip. As written in eq. (3.6) the set $\{\alpha_j\}$ may contain repeated elements in order to account for the correct order of the poles and zeros of $S(\theta)$.[8] The function $S_\alpha(\theta)$ saturates unitarity $S_\alpha(\theta)S_\alpha(-\theta) = 1$ along the entire real line. The function $f(\theta)$ parametrizes the amount of inelasticity, see (2.13). Eq. (3.6) will play a crucial role in our discussion below so let us review its derivation.

3.2.1 Discussion of eq. (3.6)

Let us define $\phi(\theta) \equiv 2i\partial_\theta \delta(\theta)$ and consider the following dispersion relation

$$\phi(\theta) = \oint_{\partial \mathcal{C}_\theta} \frac{d\theta'}{2\pi i} \frac{\phi(\theta')}{\sinh(\theta' - \theta)} \,, \tag{3.7}$$

where $\partial\mathcal{C}_\theta$ is a closed contour encircling a region $\mathcal{C}_\theta$ where $\phi(\theta)$ is regular, i.e. such that $S(\theta)$ is holomorphic and does not vanish in $\mathcal{C}_\theta$. Next we apply Cauchy's theorem and blow the contour in eq. (3.7) to the boundary of the physical strip. In doing so, we must subtract the zeros of $S(\theta)$ in the physical strip

$$\begin{aligned} \phi(\theta) = & \sum_j \left(\frac{1}{\sinh(\alpha_j - \theta)} + \frac{1}{\sinh(i\pi - \alpha_j - \theta)} \right) \\ & + \int_{-\infty}^{\infty} \frac{d\theta'}{2\pi i} \frac{\phi(\theta')}{\sinh(\theta' - \theta)} + \int_{\infty + i\pi}^{-\infty + i\pi} \frac{d\theta'}{2\pi i} \frac{\phi(\theta')}{\sinh(\theta' - \theta)} \,, \end{aligned} \tag{3.8}$$

[8] In fact, for our particular physical set up with a single stable particle $\prod_j S_{\alpha_j}(\theta)$ has no poles in the physical strip but only zeros.

JHEP09(2018)052

where the $\theta = 0, i\pi$ lines are approached from above and below, respectively. In eq. (3.8), zeros come in pairs related by crossing $S(\theta) = S(i\pi - \theta)$ and we have dropped the contribution from the contour arcs at infinity. This can be justified by assuming that $S(\theta)$ is polynomially bounded.[9] Crossing symmetry implies $\phi(\theta + i\pi) = \phi(-\theta)$. Therefore, the last integral in eq. (3.8) can be written as $\int_{-\infty}^{\infty} \frac{d\theta'}{2\pi i}\, \phi(-\theta')/\sinh(\theta' - \theta)$ and we are led to

$$\phi(\theta) = \sum_j \left(\frac{1}{\sinh(\alpha_j - \theta)} + \frac{1}{\sinh(i\pi - \alpha_j - \theta)} \right) - \int_{-\infty}^{\infty} \frac{d\theta'}{2\pi i} \frac{\partial_{\theta'} \log f(\theta')}{\sinh(\theta' - \theta)}\,, \tag{3.9}$$

where we have used $\phi(\theta) + \phi(-\theta) = \partial_\theta \log f(\theta)$, by eq. (2.13). Finally, integrating by parts with respect to θ' the integral in eq. (3.9) and using $S(\theta) = \exp \int d\theta \phi(\theta)$ we are led to eq. (3.6).

A key point of eq. (3.6) is that the roots $\{\alpha_j\}$ of the S-matrix are factored out. The factor in eq. (2.10) shows that each zero α_j in the physical strip has an accompanying pole located at $-\alpha_j$ in the unphysical strip $\mathrm{Im}\,\theta \in (-\pi, 0)$. Note however, that this observation does not necessarily imply that each zero α_j of the S-matrix in eq. (3.6) has a pole at $-\alpha_j$. Eq. (3.6) only applies in the physical strip. In order to analytically continue eq. (3.6) into the unphysical strip we need to know the nature of the branch point singularities on the real line. If the two-particle threshold branch point at $s = 4m^2$ is a square-root singularity (in the Mandelstam s-plane), then the conformal map $s = 4m^2 \cosh^2(\theta/2)$ resolves the singularity and we can analytically continue eq. (3.6) provided we avoid other possible branch points on the real line. Then we may conclude that $S(\theta)$ has poles in the unphysical strip at the same positions as the factors $S_{\alpha_j}(\theta)$. But again, this conclusion is not strictly necessary.

Even if we can analytically continue the function eq. (3.6) across the branch points on the real line, the poles of $S_{\alpha_j}(\theta)$ may be canceled by the exponential factor $\sim e^{\int \log f/\sinh}$ in eq. (3.6), which at the same time can generate poles in unphysical sheets reached by traversing higher particle production branch cuts not related to the two-particle branch point.

3.2.2 The bound

Consider a generic point $\theta = \tilde{\theta} + it$, with $\tilde{\theta} \in \mathbb{R}$ and $t \in (0, \pi)$ in the physical strip. Then, the absolute value of the S-matrix is given by

$$|S(\theta)| = \prod_j |S_{\alpha_j}(\theta)| \exp\left(\sin t \int_{-\infty}^{+\infty} \frac{d\theta'}{2\pi} \frac{\cosh(\tilde{\theta} - \theta')}{|\sinh(\theta - \theta')|^2} \log f(\theta') \right)\,, \tag{3.10}$$

where we have used $\mathrm{Re}[i \sinh^*(\theta - \theta')] = \sin t \cosh(\tilde{\theta} - \theta')$. Note that $\log f(\theta) \leqslant 0$ in the whole integration domain because $0 \leqslant f(\theta') \leqslant 1$ on the real line. Therefore we have

$$|S(\theta)| \leqslant \prod_j |S_{\alpha_j}(\theta)|\,, \tag{3.11}$$

[9] We need this kind of technical assumption to prove eq. (3.6). However, as discussed in section 3.2.3 below, this assumption is not crucial for the bound on the S-matrix that we are about to derive.

JHEP09(2018)052

for θ in the physical strip. Eq. (3.10) applies in the whole physical θ-strip and in particular it implies

$$|S'(\alpha_i)| \leqslant |S'_{\alpha_i}(\alpha_i)| \prod_{j\neq i} |S_{\alpha_j}(\alpha_i)|\,, \tag{3.12}$$

at the position of each zero α_i in the physical strip.

We shall see in section 3.3 that there is a direct relation between $|S'(\alpha_i)|$ and the parameter controlling the perturbative expansion, i.e. the dimensionless coupling constant. More precisely, we will show that $S'(\alpha_i)$ is proportional to the ratio of the expansion parameter and the square of the width of the resonance. Thus, for a fixed width and with an abuse of language, we will call

$$S'(\alpha_i)\text{: } \textit{coupling to the resonance } \alpha_i\,, \tag{3.13}$$

without reference to the actual underlying coupling constants of the possible Lagrangian description.

3.2.3 Further comments on the bound

The derivation of (3.11) presented above explicitly accounts for inelasticity $f(\theta)$ and knowledge of $f(\theta)$ results in a stronger bound than (3.11). Note, however, that the bound can be obtained in a more general setting as follows. Consider the nowhere-vanishing function

$$h(\theta) = S(\theta)/\prod_j S_{\alpha_j}(\theta)\,, \tag{3.14}$$

where the product in the denominator runs over all zeros of $S(\theta)$ with the appropriate order. By construction, $h(\theta)$ is a holomorphic function in the physical strip and is bounded on the boundaries $\operatorname{Im}\theta_b = 0, \pi$, since $|S_{\alpha_k}(\theta_b)| = 1$ and $|S(\theta_b)| \leqslant 1$. Therefore, by the Hadamard three-lines theorem, $|h(\theta)|$ is bounded in the physical strip by its value at the boundary and we are led to eq. (3.11). In refs. [10, 21] a similar argument is used to bound the residue of the poles of $S(\theta)$ on the $\theta \in [0, i\pi)$ segment in the physical strip which are associated with stable particles.

The simple derivation of (3.11) given above does not require the S-matrix to admit a representation of the form (3.6). As an example of such an S-matrix of broad interest, consider

$$S_g(\theta) = e^{2g\sqrt{\cosh^2(\theta/2)}\sqrt{1-\cosh^2(\theta/2)}} \equiv e^{ig\sinh\theta}\,, \tag{3.15}$$

where $g \geqslant 0$. The S-matrix (3.15) does not admit a representation of the form (3.6) with *finitely many factors* of S_α. In fact one can check the above S-matrix can be obtained in the limit where we have an infinite product of S_α factors [19]:

$$e^{ig\sinh\theta} = \lim_{n\to\infty} (-1)^n \prod_{j=1}^{n} S_\alpha(\theta) \tag{3.16}$$

where S_α is given by (2.10) with $\sinh\alpha = 2in/g$. The S-matrix $S_g(\theta)$ has infinitely many phase-shifts of the type in eq. (3.3) that can be interpreted as resonant particles [22].

JHEP09(2018)052

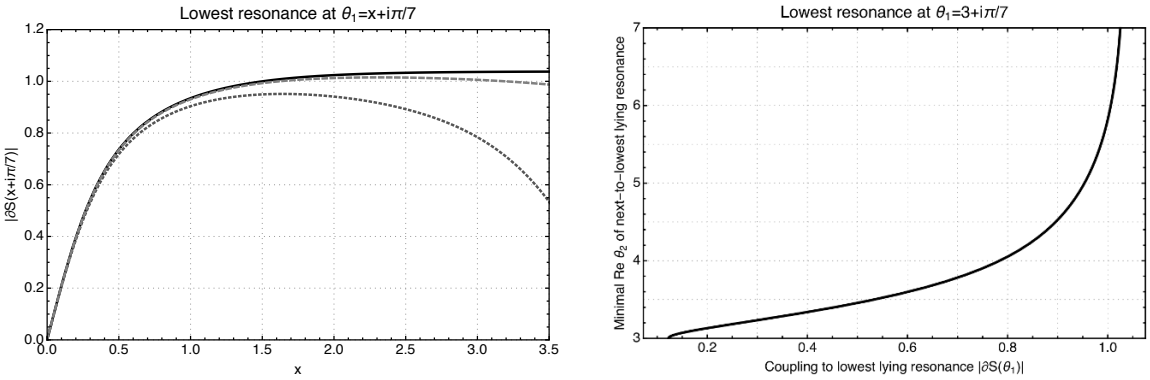

Figure 3. In the left plot, maximal coupling to the lowest mass resonance at $\theta_1 = x + i\pi/7$ for an S-matrix with a single resonance (solid black), and an S-matrix with a second resonance at $\theta_2 = 6 + i\pi/9$ (dashed light gray) and $\theta_2 = 4 + i\pi/9$ (dotted darker gray). On the right, minimal value of $\mathrm{Re}\,\theta_2$ as a function of the coupling to the θ_1 resonance for an S-matrix with two resonances.

This is easily explained from the infinite-product representation above: each S_α factor accounts for a pair of (simple) zeros in the physical strip[10] giving rise to a phase shift of 2π. In the limit $n \to \infty$ in (3.16) we end up with an infinite number of coincident zeros at $\theta = \infty + i\pi/2$, and the total (integrated) phase shift is infinite.[11] The S-matrix in (3.15) can be viewed as an integrable deformation [19, 22, 25] corresponding to the upward flow generated by certain irrelevant operators (in the RG sense). Moreover, a special limit of (3.15), namely $\lim_{g\to 0} S_g$, appears in the context of the effective string description of Yang-Mills flux tubes [26].

Eq. (3.11) implies that an S-matrix *with at least n zeros* at $\{\alpha_j\}$ has a magnitude less than or equal to $\prod_{j=1}^n |S_{\alpha_j}(\theta)|$, with $|S_\alpha(\theta)| \leqslant 1$ for θ in the physical strip. Therefore, we do not necessarily need to know the spectrum of unstable resonances up to arbitrarily high energy in order to obtain a meaningful bound. Additional knowledge of UV resonances makes the bound more stringent. This observation is key for the bounds in (3.11)–(3.12) to be sensible from an effective low energy physics standing point where we do not necessarily want to commit to a particularly detailed spectrum of UV resonances beyond a certain energy cutoff. To illustrate this point we have plotted $|S'(\theta_1)|$ as a function of $x \equiv \mathrm{Re}\,\theta_1$ for the S-matrix $S_1 = S_{\theta_1} S_{-\theta_1^*}$ (black solid line) in the left plot in figure 3. Any other theory which features resonances at $\{\theta_1, -\theta_1^*\}$ has a coupling $|S'(\theta_1)|$ which falls below this line. For comparison, the same plot depicts $|S'(\theta_1)|$ for the S-matrix $S_2 = S_{\theta_1} S_{-\theta_1^*} S_{\theta_2} S_{-\theta_2^*}$ featuring a second pair of resonances at $\{\theta_2, -\theta_2^*\}$. The dotted line depicts $|S_2'(\theta_1)|$ for $\theta_2 = 4 + i\pi/9$ and the dashed line is plotted with $\theta_2 = 6 + i\pi/9$. As can be seen from the plots the closer the resonances are to each other the stricter the bound on $|S'(\theta_1)|$ gets. Thus, the effects of possible further heavy resonances $|\theta_1 - \theta_j| \gg 1$ decouples at low energy.

The latter observation suggests another interesting viewpoint on the bound (3.12): the larger the value of $|S'(\theta_1)|$, the larger the minimum mass gap with the nearest resonance θ_2.

[10] Higher order zeros can be factorized by point-splitting, $S_\alpha^n = \prod_{j=1}^n S_{\alpha+j\epsilon}$, where $\epsilon \sim e^{-n}$.

[11] Other examples with infinitely many resonances are the elliptic (doubly periodic) S-matrix such as refs. [23, 24].

JHEP09(2018)052

Namely, the mass gap increases monotonically as $|S'(\theta_1)|$ increases. This is illustrated in the right plot of figure 3 for $S = S_{\theta_1} S_{-\theta_1^*} S_{\theta_2} S_{-\theta_2^*}$ with $\theta_1 = 3 + i\pi/7$ and $\mathrm{Im}\,\theta_2 = i\pi/9$ held fixed. The black line vanishes at a positive value of $S'(\theta_1)$ because below a critical coupling there is no bound on the mass gap for a system with only two resonances $\{\theta_1, \theta_2\}$. Further assumptions on the spectrum of possible higher mass resonances would lead to stricter bounds on the separation $\mathrm{Re}\,\theta_1 - \mathrm{Re}\,\theta_2$.

3.3 Interpretation of the bound

Consider an effective action describing the low energy dynamics of two massive scalar fields with a cubic interaction in two dimensions,

$$S = \int \mathrm{d}^2x \left[\frac{1}{2} \left(\partial^\mu \pi \partial_\mu \pi - m^2 \pi^2 + \partial^\mu \sigma \partial_\mu \sigma - M^2 \sigma^2 \right) - \frac{\lambda}{2} \sigma \pi^2 - \dots \right] , \tag{3.17}$$

where $\cdots$ denote further interactions of the fields that stabilize the potential at large field values but whose coupling constant is much smaller than λ/m^2 and are therefore inconsequential for the discussion below.

3.3.1 Perturbative S-matrix

Due to the cubic vertex in (3.17), for $M > 2m$ the particle excitations of σ are unstable and can decay to lighter particles. This instability manifests itself as a resonance in the $\pi\pi \to \pi\pi$ scattering which can be analyzed with perturbation theory. The $\pi\pi \to \pi\pi$ component of the S-matrix is given by[12]

$$\mathbf{S} = S(s)\,\mathbb{1} = \left(1 + \frac{i\mathcal{M}(s)}{2\sqrt{s}\sqrt{s-4m^2}} \right) \mathbb{1} \tag{3.18}$$

where the identity is the inner product of two particle states $\mathbb{1} = \langle p_3, p_4 | p_1, p_2 \rangle$. The amplitude $\mathcal{M}$ is given by the sum of the σ-exchange diagrams in the s, t and u-channel:

$$i\mathcal{M}(s) =$$ 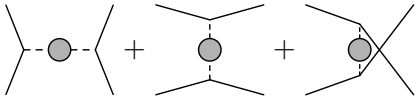 $$.$$ (3.19)

Up to higher order loop corrections and non-perturbative effects $\mathcal{M}$ is given by

$$\mathcal{M}(s) = \frac{\lambda^2}{M^2 + \frac{\lambda^2}{8\pi m^2}} - \frac{\lambda^2}{s - M^2 - \Pi(s)} - \frac{\lambda^2}{4m^2 - s - M^2 - \Pi(4m^2 - s)} , \tag{3.20}$$

where $\Pi(s)$ is the (amputated) two-point function given by

$$\Pi(s) = \frac{\lambda^2}{2\pi} \frac{\tanh^{-1} \sqrt{\frac{s}{s-4m^2}}}{\sqrt{s(s-4m^2)}} . \tag{3.21}$$

As discussed in section 2, we find that eq. (3.18) is crossing symmetric $S(s) = S(4m^2 - s)$, it is analytic in the domain $0 < |s \pm i\epsilon| < 4m^2$ and real along the real line in that domain.

[12] See appendix C for details.

JHEP09(2018)052

At the two-particle production threshold $s = 4m^2$ there is a square-root branch point and by crossing symmetry we find another one at $s = 0$.

It is convenient to resolve the square-root singularities at $s = 0, 4m^2$ by means of the conformal map in eq. (2.8). Henceforth we work in units such that $m = 1$. As a function of θ, the S-matrix in (3.18) is single-valued and given by

$$S(\theta) = 1 + \frac{i\lambda^2}{4\sinh\theta}\left[\frac{1}{M^2 + \frac{\lambda^2}{8\pi}} - \frac{1}{4\cosh^2\left(\frac{\theta}{2}\right) - M^2 - \Pi(\theta)} + \frac{1}{4\sinh^2\left(\frac{\theta}{2}\right) + M^2 + \Pi(i\pi - \theta)}\right], \tag{3.22}$$

where the amputated two-point function is given by

$$\Pi(\theta) = \frac{\lambda^2}{8\pi}\frac{\theta - i\pi}{\sinh\theta}, \tag{3.23}$$

for θ in the fundamental domain $\theta \in (-i\pi, i\pi]$.[13]

3.3.2 Zeros and poles

For $M > 2$ the S-matrix in eq. (3.22) has four poles and four zeros. The two s-channel poles are located at

$$\theta_p^{\pm} = \pm\left(\theta_\circ + \frac{\lambda^2\theta_\circ}{16\pi\sinh^2\theta_\circ}\right) - \frac{i\lambda^2}{16\sinh^2\theta_\circ}, \tag{3.24}$$

where $\theta_\circ = 2\cosh^{-1}\left(\frac{M}{2}\right)$, and the two zeros are located at

$$\theta_z^{\pm} = \pm\left(\theta_\circ + \frac{\lambda^2\theta_\circ}{16\pi\sinh^2\theta_\circ}\right) + \frac{i\lambda^2}{16\sinh^2\theta_\circ}, \tag{3.25}$$

in the physical strip. Note that $\theta_z^{\pm} = -\theta_p^{\mp}$, as required by unitarity. The location of the remaining poles and zeros follow from crossing symmetry, i.e. $S(\theta) = S(i\pi - \theta)$, and are located at

$$\theta_{p/z}^{c\,\pm} = i\pi - \theta_{p/z}^{\pm}. \tag{3.26}$$

Let us remark that the zeros $\{\theta_z^{\pm}, \theta_z^{c\,\pm}\}$ lie above the real axis corresponding to the physical sheet while the poles $\{\theta_p^{\pm}, \theta_p^{c\,\pm}\}$ lie below the real axis corresponding to the second Riemann sheet of the $s = 0, 4m^2$ branch points. Thus, the picture is qualitatively similar to the one depicted in figure 2.

3.3.3 Bound

In order to better understand the scope of the bound (3.12) lets consider it in the context of the perturbative example. Near the root at $\theta = \theta_i$ one of the denominators in the perturbative S-matrix (3.22) is of order λ^2, see appendix C for details. Consequently the dominant contribution to $S'(\theta_i)$ goes like λ^{-2}. For $\theta_i = \theta_z^{\pm}$ given by (3.25) we find

$$S'(\theta_i) = -\frac{2i}{\lambda^2}M^2(M^2 - 4) + O(\lambda^0), \tag{3.27}$$

[13] Eq. (3.23) is valid in the fundamental domain $\theta \in (-i\pi, i\pi]$. However, it can be extended to the entire complex θ-plane by means of the identity $\theta - i\pi = \log\left(\frac{\sinh\theta/2 - \cosh\theta/2}{\sinh\theta/2 + \cosh\theta/2}\right)$, valid in the fundamental domain, where the r.h.s. is periodic in the imaginary axis direction with period $\theta \sim \theta + 2\pi i$.

JHEP09(2018)052

thus eq. (3.12) bounds $\sim M^4/\lambda^2$ (in units of $m = 1$). The width of the resonance associated to θ_i is given by

$$\Gamma = -\operatorname{Im}\Pi(\theta_\circ)/M = \lambda^2/(4M^2\sqrt{M^2-4}) \tag{3.28}$$

and hence $S'(\theta_i)$ can be expressed as

$$|S'(\theta_i)| = \frac{\lambda^2}{8M^2\Gamma^2}\,. \tag{3.29}$$

Note that at this order in perturbation theory the effective perturbative parameter is given by $\lambda_{\text{eff}} = \frac{\lambda}{M}$ (as can be seen in (3.22)). In light of this observation, eq. (3.29) can be interpreted as follows: for a resonance particle σ with a fixed width Γ, the strength of the coupling between σ and the stable particles π is constrained to obey bound (3.12). This indicates that for fixed width, $|S'(\theta_i)|$ is directly related to the coupling parameter of the stable particles to the resonance particle θ_i and can therefore be (loosely) referred to as the coupling. We remark that the bound is saturated at this order of perturbation theory, and that higher order corrections set $|S'(\theta_i)|$ within the bound due to particle production $S_{2\to4} > 0$.

4 Numerical optimization

The results presented in the previous section do not admit a straightforward generalization to higher dimensions where the analytical approach proves cumbersome. For this reason here we present an alternative approach utilizing numerical methods which can be generalized to higher dimensions. This approach can be summarized in two key steps. First, we construct an ansatz for the S-matrix which encodes analyticity and crossing symmetry as well as the location of the unstable resonances. The free parameters of the ansatz include the resonance coupling parameters. The second step is to maximize these coupling parameters under the constraint of unitarity $S(\theta)S(-\theta) \leqslant 1$ thus recovering the analytical bound of the previous section.

In $1+1$ dimensions the $2 \to 2$ S-matrix element admits a simple expansion which we can exploit to build our ansatz. Although this ansatz does not generalize to higher dimensions it serves as a simple framework to demonstrate how the numerical approach outlined above is implemented. Thus we first present the numerical approach using this ansatz before presenting a more general ansatz which can readily be generalized to higher dimensions.

4.1 A simple S-matrix ansatz for $d = 1+1$

Let us denote by $S_{\text{ans}}^{\{\theta_j\}}$ our ansatz for the $2 \to 2$ S-matrix element. This ansatz is labelled by the location of its roots in the θ-strip $\{\theta_j\}$. To encode holomorphicity of the function $S_{\text{ans}}^{\{\theta_j\}}$ in a domain $\mathcal{D}_\theta$ of the θ-strip we consider a conformal map ρ from $\mathcal{D}_\theta$ into the unit disk. The S-matrix, viewed as a function of ρ, is therefore holomorphic inside the unit disk. A holomorphic function inside the unit disk is analytic and therefore admits an absolutely convergent Taylor expansion inside the disk. Thus $S_{\text{ans}}^{\{\theta_j\}}(\rho)$ can be defined via its Taylor expansion inside the unit disk which makes holomorphicity of $S_{\text{ans}}^{\{\theta_j\}}(\rho(\theta))$ in $\mathcal{D}_\theta$ manifest.

JHEP09(2018)052

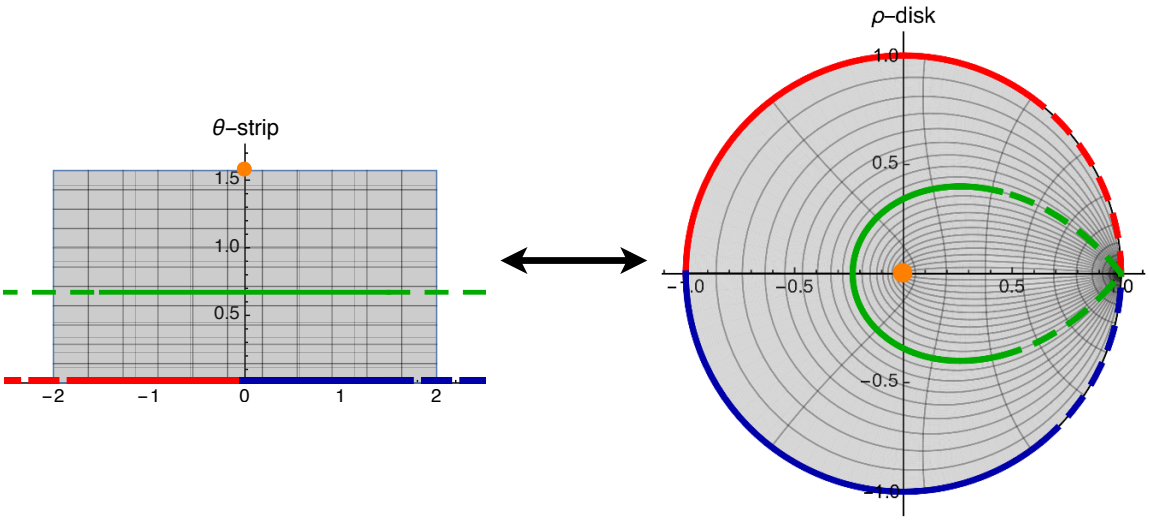

Figure 4. Illustration of the conformal map in eq. (4.1) with $\beta = i\pi$.

To make crossing symmetry $S_{\text{ans}}^{\{\theta_j\}}(\theta) = S_{\text{ans}}^{\{\theta_j\}}(i\pi - \theta)$ manifest we require the map $\rho(\theta)$ to satisfy $\rho(\theta) = \rho(i\pi - \theta)$. Such a map can be viewed as a biholomorphic map between the fundamental domain $\text{Im}\,\theta \in (0, \pi/2)$ and the unit disk. A conformal map with such properties is given by

$$\rho(\theta) = \frac{\sinh\theta - i}{\sinh\theta + i}\,. \tag{4.1}$$

As illustrated in figure 4, under the map eq. (4.1) the crossing symmetric point $\theta = i\pi/2$ is mapped into the origin of the disk while the real axis is mapped to the boundary.

Since we require that the ansatz vanishes at $\rho_{\theta_i} = \rho(\theta_i)$, the function

$$g(\rho) \equiv S_{\text{ans}}^{\{\theta_j\}}(\rho) / \prod_j (\rho - \rho_{\theta_j}) \tag{4.2}$$

is nowhere vanishing and holomorphic inside the unit disk and therefore admits an absolutely convergent Taylor expansion

$$g(\rho) = z\left(1 + \sum_{n=1}^{\infty} c_n \rho^n\right)\,, \tag{4.3}$$

where the overall factor is given by $z \equiv g(0) > 0$.

Combining (4.2) and (4.3) results in the following representation of our ansatz S-matrix element

$$S_{\text{ans}}^{\{\theta_j\}}(\rho) = z \prod_j (\rho - \rho_{\theta_j}) \left(1 + \sum_{n=1}^{\infty} c_n \rho^n\right)\,, \tag{4.4}$$

which is holomorphic, crossing symmetric and encodes the location of the zeros ρ_{θ_j}. The parameters $\{z, c_i\}$ are constrained by unitary of the S-matrix eq. (4.5) but are otherwise arbitrary real parameters.

Our next step is to maximize z over the space of the expansion coefficients $\{c_n\}$ in eq. (4.4) under the constraint of unitarity. The unitarity bound along the real line in the

JHEP09(2018)052

θ-strip translates to an analogous bound along the boundary of the unit disk parameterized as $\rho = e^{i\phi}$,

$$S_{\text{ans}}^{\{\theta_j\}}(e^{i\phi})\, S_{\text{ans}}^{\{\theta_j\}}(e^{-i\phi}) \leqslant 1 \qquad \text{for} \quad \phi \in [0,\pi]\,. \tag{4.5}$$

Maximizing over z is tantamount to maximizing over the coupling to the resonances $\partial_{\theta_k} S_{\text{ans}}^{\{\theta_j\}}(\rho_{\theta_k})$, with the location of the roots of $S_{\text{ans}}^{\{\theta_j\}}$ held fixed. All couplings are maximized simultaneously, as follows from (3.12).

4.1.1 Numerical results

In order to set up the numerical code to maximize over z, the series in (4.4) has to be truncated. Therefore in the numerical code we maximize z in the truncated ansatz

$$S_{\text{M}}^{\{\theta_j\}}(\rho) = z \prod_j (\rho - \rho_{\theta_j}) \left(1 + \sum_{n=1}^{M} c_n \rho^n\right) . \tag{4.6}$$

In addition, the constraint (4.5) is imposed in a large but finite number of points on the unit circle, namely it is evaluated at K points

$$\phi \in \{0, \pi/K, 2\pi/K, \ldots, \pi\} \ . \tag{4.7}$$

The only approximation made in this implementation is in the truncation of the series in (4.6). Convergence as M is increased is fast and even keeping the first few terms leads to precise results.

As an example, consider

$$\{\theta_j\} = \{3+i, -3+i\}\,, \tag{4.8}$$

in eq. (4.6). We maximize (4.6) over z under the unitary constraint for the set of zeros in (4.8) and we get the white lines depicted in figure 5. To obtain such result we increased M and K until we got a convergent result, the plots shown are for $\{M, K\} = \{60, 90\}$. The white lines are super-imposed over black thicker lines. These correspond to the S-matrix theory S_{ex} of (3.5) with $\alpha \to 3+i$

$$S_{\text{ex}}(\theta) = S_{3+i}(\theta) S_{-3+i}(\theta)\,, \tag{4.9}$$

in the left plot, while in the right plot we compare with the phase-shift of S_{ex}.[14] The numerical results have been obtained with `Mathematica`'s function `FindMaximum`. The computation is cheap, taking $O(1)$ min. of time and ~ 1 Mb of memory RAM. Optimization of S-matrices with many more resonances is also feasible and leads to equally good results.

[14] Recall that S_{ex} saturates unitarity at all physical energies. In $d = 3+1$, only the trivial S-matrix saturates unitarity at all energies, since any non-trivial S-matrix has a finite amount of particle production. From this perspective, wether or not we can identify a Lagrangian model leading to S_{ex} is somewhat anecdotic and special to $d = 1+1$ physics.

JHEP09(2018)052

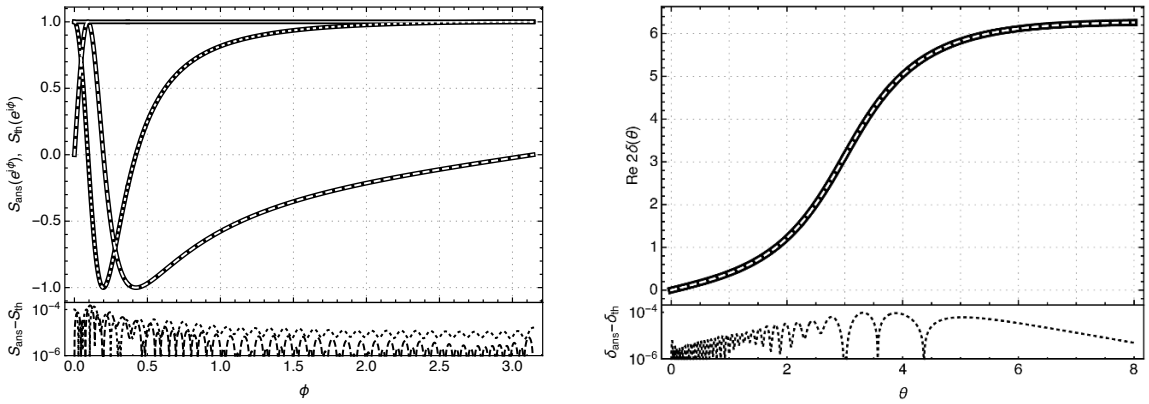

Figure 5. In the left plot solid black lines depict the imaginary part, real part and absolute value of $S_{\rm th}(e^{i\phi})$. Superimposed we show the imaginary part (dashed white), the real part (doted white) and absolute value (solid white) of $S_{\rm ans}(e^{i\phi})$. In the lower left plot, sharing the same horizontal axis, we show the real part (dotted) and the imaginary part (dashed) of $S_{\rm th}(e^{i\phi})-S_{\rm ans}(e^{i\phi})$. Finally the plot to the right is a comparison of the phase of $S_{\rm ans}$ (white) and $S_{\rm th}$ (black) in the θ strip.

4.2 Towards generalization to higher dimensions

It is convenient to make crossing symmetry explicit by extending S into a symmetric function of two Mandelstam variables $S(s,t) = S(t,s)$. An ansatz of this form is much more suitable for generalization to higher dimensions. In $1+1$ dimensions the physical S-matrix is obtained by constraining $S(s,t)$ to the plane $s+t = 4m^2$. This function is analytical in s and t up to the branch points on the real line.

Next, we build an ansatz $S^{\{\omega_i\}}_{\text{ans-2}}(s,t)$ encoding analyticity, crossing, and the location of the resonances. Similar to what we did in section 4.1 we encode analyticity in each variable s and t by conformally mapping the domain of holomorphicity into the unit disk and subsequently define the function as a Taylor series in the poly-disk. Such a conformal map is provided by

$$\omega(s) = \frac{\sqrt{2m^2} - \sqrt{4m^2 - s}}{\sqrt{2m^2} + \sqrt{4m^2 - s}}\,. \tag{4.10}$$

As we did before, we factor out the zeros of $S^{\{\omega_i\}}_{\text{ans-2}}(s,t)$, and expand the nowhere vanishing part in a (convergent) double-expansion whilst fulfilling all the physical assumptions,

$$S^{\{\omega_i\}}_{\text{ans-2}}(s,t) = z \prod_i \left[\omega_i - \omega(s)\right]\left[\omega_i - \omega(t)\right] \left(1 + \sum_{m,n=1}^{\infty} c_{n,m}\, \omega(s)^n \omega(t)^m\right)\,. \tag{4.11}$$

Here $c_{m,n}$ are symmetric and real. Eq. (4.11) can be equivalently written in the corresponding θ_s, θ_t-strips. The existence of such a double expansion eq. (4.11) is easy to show in two dimensions. To this end note that the map (4.1), with $\theta = 2\cosh^{-1}\left(\frac{\sqrt{s}}{2m}\right)$, has the following convergent expansion

$$\rho(s) = \left[\omega(s) + \omega(4m^2 - s)\right] \sum_{n=0}^{\infty} (-1)^n\, \omega(4m^2 - s)^n\, \omega(s)^n\,.$$

This, together with (4.4), results in the double expansion (4.11) with $t = 4m^2 - s$.

JHEP09(2018)052

Evaluating $S^{\{\omega_i\}}_{\text{ans-2}}(s,t)$ at $t = 4m^2 - s$, and maximizing over z under the unitarity constraint we obtain comparable results to the ones showed in figure 5. Eq. (4.11) admits a generalization from $d = 1+1$ to $d = 3+1$ spacetime dimensions as was done in [10]. In $d = 3+1$ there is an analogous definition of resonance presented in section 3.1, in terms of phase-shifts and roots of the components of the S-matrix in the partial wave decomposition. In a forthcoming publication we plan to study the space of S-matrices in $d = 3+1$ that feature unstable resonances.

5 Summary and outlook

In this work we have found a bound on the coupling of asymptotic states to unstable resonances, eq. (3.12), which is saturated in the limit of maximal elasticity of the $2 \to 2$ S-matrix element. The bound for each resonance is improved as the number of resonances is increased, or the gap between the resonances is decreased. Therefore (3.12) can be interpreted as setting a minimal mass gap between the resonances as a function of the coupling to the resonances. In section 4 we have recovered the analytical results of section 3 as a numerical solution. This consists in numerically maximizing the coupling to the resonances of the S-matrix ansatz (4.6) or (4.11) under the constraint of unitarity.

There are a number of interesting directions left to be developed. For instance, in $d = 1+1$ spacetime dimensions, generalizing our results to systems involving many non-trivial $2 \to 2$ S-matrix elements is of interest and could prove instructive for more involved problems in higher dimensions. This would also facilitate making contact with integrable models such as ref. [27] which have a known Lagrangian description and feature unstable particles. Another interesting direction in $d = 1+1$ is to constrain unstable resonances by studying the crossing symmetry constraints on four-point functions in the boundary of AdS in $d = 1+1$ and subsequently taking the flat space limit [8].

Perhaps the most promising direction to pursue, from the particle physics point of view, is to generalize the results obtained here to $d = 3+1$. In section 4 we have explained a possible route towards such generalization. This avenue promises many applications to particle physics and model building beyond the Standard Model. It would also be interesting to study unstable particles of higher spin in the $2 \to 2$ scalar S-matrix element which can be achieved via incorporating the corresponding Legendre polynomials in the S-matrix ansatz.

A naive generalization of the bound (3.12) to $d = 3+1$ suggests that we should find a maximal value of $|S'|$ for unstable resonances which is saturated in the limit where the amount of particle production is minimized. Furthermore, we anticipate an interesting interplay between the maximal value of $|S'|$ and the number of resonances allowed below a given energy. For instance, in analogy to the result of section 3.2.3, in $d = 3+1$ we expect that given the value $S'(\theta_i)$ of the lightest resonance there is a lower bound on the mass of the next-to-lowest lying resonance.

JHEP09(2018)052

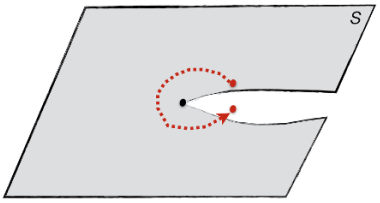

Figure 6. Analytic continuation of eq. (2.5) through the branch cut.

Acknowledgments

We thank G. Mussardo, S. Rychkov, B. van Rees and G. Villadoro for the useful discussions. We are also grateful to J. Penedones, M. Serone and L. Vitale for the useful discussions and comments on the draft. N.D. is supported by the PRIN project "Non-perturbative Aspects Of Gauge Theories And Strings".

A Nature of the two-particle branch point

Eq. (2.5) can be used to argue that the two-particle threshold branch point is a square-root singularity, see for instance [28]. The argument goes as follows. Consider the analytical continuation of $S(s+i\epsilon)$ into the second Riemann sheet by following a full anti-clockwise rotation around $s=4m^2$, see figure 6. Lets call such analytically continued function $G(s)$. Then, under such analytical continuation, the unitary equation becomes

$$S(s-i\epsilon)G(s-i\epsilon)=f(s)\,, \tag{A.1}$$

where we made use of continuity $S(s-i\epsilon)=G(s+i\epsilon)$ (and assumed that $f(s)$ has no branch points). Then, by taking the ratio between eq. (2.5) and eq. (A.1) one obtains

$$G(s-i\epsilon)=S(s+i\epsilon)\,. \tag{A.2}$$

The latter equation would imply that rotating around the two-particle branch point twice the S-matrix is invariant. Therefore, if the S-matrix has a branch point and if the branch point is an algebraic singularity then it must be a square-root type singularity.[15] A similar result can be obtained in $d=3+1$ dimensions [13].

B Total integrated phase-shift

The function $S(\theta)$ is meromorphic inside the physical strip $\mathrm{Im}\,\theta\in(0,\pi)$. The so called *argument principle* implies[16]

$$\oint_{\partial P}\frac{d\theta}{2\pi i}\,\partial_\theta(2i\delta(\theta))=N_z-N_p\,. \tag{B.1}$$

[15] Note that this argument alone can not exclude the possibility of two-sheeted essential singularities.
[16] See for instance theorem 4.1 of [29].

JHEP09(2018)052

where the closed contour integral encircles some region P in the physical strip and N_z and N_p are the number of zeros and poles in that region, weighted by their order. In our particular physical set up P is inside the physical θ-strip and thus there are no poles ($N_p = 0$) due to stable particles.

Now, using crossing symmetry we have $\partial_\theta \delta(i\pi + \theta) = -\partial_\theta \delta(-\theta)$ and therefore the total phase-shift can be written as a contour integral

$$\int_{-\infty}^{\infty} d\theta\, \partial_\theta \delta(\theta) = \frac{1}{2} \oint_{\mathcal{C}} d\theta\, \partial_\theta \delta(\theta)\,, \tag{B.2}$$

with $\mathcal{C}$ is a contour encircling the whole physical strip. Then, by Cauchy residue theorem, (3.2) follow from (B.2). For simplicity we have assumed that $S(\theta)$ asymptotes to a constant at $\theta \to \pm\infty$ so that the contribution from the segments at infinity vanishes — this assumption can be relaxed.

C Perturbative example

In this appendix we provide further details of the perturbative QFT discussed in section 3.3. The Feynman rules for the theory in (3.17) are

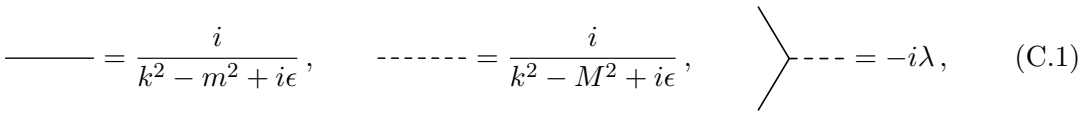

(C.1)

where the plain line denotes the propagator for π and the dashed line denotes the propagator for σ. First order of business is to compute the loop corrections to propagation of σ which is captured by the (amputated) diagram

(C.2)

The loop integral can be carried out explicitly and yields

$$\Pi(k^2) = \frac{i}{2}(-i\lambda)^2 \int \frac{\mathrm{d}^2 q}{(2\pi)^2} \frac{i}{q^2 - m^2 + i\epsilon} \frac{i}{(k-q)^2 - m^2 + i\epsilon} = \frac{\lambda^2}{2\pi} \frac{\tanh^{-1}\sqrt{\frac{k^2}{k^2 - 4m^2}}}{\sqrt{k^2}\sqrt{k^2 - 4m^2}}\,, \tag{C.3}$$

where the limit $\epsilon \to 0$ was taken in the integrated function. Along the real axis and below the two-particle threshold $k^2 < 4m^2$ the loop correction $\Pi(k^2)$ is real. Above the two-particle threshold $\Pi(k^2)$ has a non-vanishing imaginary part

$$\mathrm{Im}\,\Pi(k^2) = -\frac{\lambda^2}{4\sqrt{k^2(k^2 - 4m^2)}}\, \theta(k^2 - 4m^2)\,. \tag{C.4}$$

The latter equation can be extracted directly using Cutkosky rules.

JHEP09(2018)052

C.1 The perturbative S-matrix

Incorporating the loop correction to the propagator (C.3), the quantum corrected propagator for σ is given by

$$\mathcal{G}(k^2) \; = \; \text{---}\bigcirc\text{---} \; = \frac{i}{k^2 - M^2 - \Pi(k^2) + i\epsilon} \,. \tag{C.5}$$

With this propagator we can readily compute the $\pi\pi \to \pi\pi$ component of the S-matrix. The contributing diagram in the s-channel is

$$\rangle\text{-}\bigcirc\text{-}\langle \; = \frac{-i\lambda^2}{s - M^2 - \Pi(s) + i\epsilon} \; = \; -\lambda^2 \mathcal{G}(s) \tag{C.6}$$

where $s = (p_1 + p_2)^2$. In the centre of mass frame we have $p_1 = p_4 = (p^0, p^1)$ and $p_2 = p_3 = (p^0, -p^1)$. Thus $t = (p_1 - p_3)^2 = 4m^2 - s$ and $u = (p_1 - p_4)^2 = 0$. The corresponding amplitude in the t-channel amounts to $-\lambda^2\mathcal{G}(t) = -\lambda^2\mathcal{G}(4m^2 - s)$ and the u-channel diagram yields a contribution equal to $-\lambda^2\mathcal{G}(u) = -\lambda^2\mathcal{G}(0)$. The one-loop amplitude — up to higher order corrections[17] — is given by

$$i\mathcal{M}(s) = \frac{i\lambda^2}{M^2 + \frac{\lambda^2}{8\pi m^2}} - \frac{i\lambda^2}{s - M^2 - \Pi(s)} - \frac{i\lambda^2}{4m^2 - s - M^2 - \Pi(4m^2 - s)} \,. \tag{C.7}$$

Then, the $\pi\pi \to \pi\pi$ component of the S-matrix is given by

$$\mathbf{S} = S(s)\,\mathbb{1} = \left(1 + \frac{i\mathcal{M}(s)}{2\sqrt{s(s-4m^2)}}\right)\mathbb{1} \tag{C.8}$$

where the identity is the inner product of two particle states $\mathbb{1} = \langle p_3, p_4 | p_1, p_2 \rangle$, which is given by

$$\mathbb{1} = (2\pi)^2 4E_1E_2 \left(\delta(p_1^1 - p_3^1)\delta(p_2^1 - p_4^1) + \delta(p_1^1 - p_4^1)\delta(p_2^1 - p_3^1)\right) \,, \tag{C.9}$$

and the extra factor multiplying $\mathcal{M}(s)$ arises from the identity $(2\pi)^2\delta^{(2)}(p_1 + p_2 - p_3 - p_4) = \mathbb{1}/(2\sqrt{s}\sqrt{s-4m^2})$.

A few remarks regarding $S(s)$ defined in (C.8) are in order. As we will demonstrate below, the above S-matrix has complex poles hidden behind a branch cut stemming from the two-particle threshold. These poles correspond to the exchange of an on-shell unstable σ particle which amounts to a resonance in the scattering process whose width is determined by

$$\Gamma = -\operatorname{Im}\Pi(M_{\text{ren}}^2)/M_{\text{ren}} \,. \tag{C.10}$$

The resonance is observed as a phase shift due to a branch cut in $\log S(s)$ stemming from such poles. Alternatively we can extract the same information about the resonance from the zeros of $S(s)$ as they too give rise to a branch cut in $\log S(s)$ and thus result in a phase shift. Moreover the zeros are in a sense more fundamental as they are not hidden behind any branch cuts and we do not need to analytically continue the S-matrix through branch cuts to study them. Below we analyze the resonance in our perturbative example first by studying the poles and later through the zeros.

[17] Namely, vertex corrections and box diagrams.

JHEP09(2018)052

C.2 Resonances, poles and zeros

As discussed in section 3.1, resonances are associated with branch cuts in the s-plane for the function $\log S(s)$ which typically connect a pair of pole and zero of the S-matrix the location and residue of which determine the features of the resonance. Here we study the zeros and poles of the perturbative S-matrix (C.8).

C.2.1 Poles in s-plane

Poles associated to unstable resonances are not visible on the complex s-plane and are hidden behind multi-particle branch cuts of the S-matrix. To illustrate this in our perturbative example note that (C.8) has square-root branch points at $s = 0$ and at $s = 4m^2$. We take the branch cuts to stretch along the real axis from $-\infty$ to 0 and from $4m^2$ to $+\infty$. The location of the poles of $S(s)$ due to the exchange of a σ in the s-channel are determined by

$$s - M^2 - \Pi(s) = 0\,. \tag{C.11}$$

Now consider the following ansatz for the solution

$$s_* = 4m^2 + s_\circ e^{i\varphi + 2\pi i n} \tag{C.12}$$

where $s_\circ$ is taken to be positive, $\varphi \in [0, 2\pi)$ and $n = 0, 1$ labels the sheets of the Riemann surface associated with the function $\sqrt{s - 4m^2}$. Plugging our ansatz into the equation (C.11) and taking the real part we obtain

$$s_\circ \cos\varphi + 4m^2 - M^2 - \mathrm{Re}\,\Pi(s_*) = 0\,. \tag{C.13}$$

This implies $s_* = M^2 + O(\lambda^2)$ and since $4m^2 - M^2 - \mathrm{Re}\,\Pi(M^2) < 0$ we must have $\varphi \in (0, \pi/2) \cup (3\pi/2, 2\pi)$. Therefore, the imaginary part of (C.11) simplifies to

$$s_\circ \sin\varphi + \frac{\lambda^2}{4}\frac{(-1)^n \cos(\varphi/2)}{M\sqrt{s_\circ}} = 0\,. \tag{C.14}$$

where we have used (C.4) and have omitted higher order terms using that $\sin\varphi = O(\lambda^2)$. It is evident that the equation has no solution for $n = 0$, i.e. in the physical sheet. To find a solution we have to take $n = 1$ which as can be seen from (C.12) corresponds to the analytic continuation of the function $\sqrt{s - 4m^2}$ into the second sheet.[18]

Having demonstrated that the poles lie behind the square-root branch cut stemming from the two-particle threshold at $s = 4m^2$ we now switch to the θ-variable, introduced in section 2.1. Recall that $\theta = \theta(s)$ maps the two-sheeted Riemann surface associated to eq. (C.8) into the strip $\theta \in [-i\pi, i\pi)$.

[18] Here we have assumed $M \geqslant 2m$. For $M < 2m$ we find a pole on the real axis and below the two-particle threshold corresponding to production of a stable particle of mass M.

JHEP09(2018)052

C.2.2 Poles and zeros of the S-matrix

The S-matrix on the θ-strip, in units $m = 1$, was given in (3.22):

$$S(\theta) = 1 + \frac{i\lambda^2}{4\sinh\theta}\left[\frac{1}{M^2+\frac{\lambda^2}{8\pi}} - \frac{1}{4\cosh^2\left(\frac{\theta}{2}\right) - M^2 - \Pi(\theta)} + \frac{1}{4\sinh^2\left(\frac{\theta}{2}\right) + M^2 + \Pi(i\pi-\theta)}\right]. \tag{C.15}$$

We remind the reader that the above expressions are perturbative results valid only up to order λ^3. We are interested in finding poles and zeros of the S-matrix in the fundamental domain of complex θ. To this end we can use a series expansion for small λ. The poles arise when one of the denominators vanishes. Since $S = 1 + O(\lambda^2)$, the zeros lie in the regions where one of the denominators is of order λ^2. Thus we can look for location of zeros and poles in parallel. The location of the zeros and poles arising from the s-channel contribution are determined by the equation

$$4\sinh\theta\,\left(4\cosh^2(\theta/2) - M^2 - \Pi(\theta)\right) = ia\lambda^2 \tag{C.16}$$

where $a = 0$ for poles and $a = 1$ for zeros.

Note that the t and u-channel contributions to (C.16) appear at order λ^4 along with contributions from other diagrams we have not considered. These contributions only affect the position of the pole and the zero at order λ^4. We are interested in poles and zeros near $s_\circ = M^2$ or $\theta_\circ^\pm = \pm 2\cosh^{-1}\left(\frac{M}{2}\right)$. We therefore look for perturbative solutions of the form

$$\theta_\sigma^\pm = \theta_\circ^\pm + \lambda^2\theta_*^\pm\,. \tag{C.17}$$

Plugging this ansatz into (C.16) we find

$$8\,\theta_*^\pm\,\sinh^2\theta_\circ^\pm - \frac{\theta_\circ^\pm - i\pi}{2\pi} = ia \tag{C.18}$$

and therefore

$$\theta_*^\pm = \frac{1}{8\sinh^2\theta_\circ^\pm}\left(\frac{\theta_\circ^\pm}{2\pi} + i\left(a - \frac{1}{2}\right)\right). \tag{C.19}$$

Thus we find two poles at

$$\theta_p^\pm = \pm\left(\theta_\circ + \frac{\lambda^2\theta_\circ}{16\pi\sinh^2\theta_\circ}\right) - \frac{i\lambda^2}{16\sinh^2\theta_\circ} \tag{C.20}$$

and two zeros located at

$$\theta_z^\pm = \pm\left(\theta_\circ + \frac{\lambda^2\theta_\circ}{16\pi\sinh^2\theta_\circ}\right) + \frac{i\lambda^2}{16\sinh^2\theta_\circ} \tag{C.21}$$

where $\theta_\circ = 2\cosh^{-1}\left(\frac{M}{2}\right)$. Note that the zeros lie above the real axis corresponding to the physical sheet while the poles lie below the real axis corresponding to the second sheet and that the location of the zeros and poles are related by

$$\theta_z^\pm = -\theta_p^\mp \tag{C.22}$$

JHEP09(2018)052

as required by unitarity. We also find a second pair of poles and zeros located at

$$\theta^{c\,\pm}_{p/z} = i\pi - \theta^{\pm}_{p/z} \tag{C.23}$$

using crossing symmetry.

We remind the reader that (C.20) and (C.21) are only valid up to corrections of order λ^4 while (C.21) only satisfy $S(\theta) = 0$ up to corrections of order λ^2. This is due to the fact that near the roots of $S(\theta)$ the s-channel denominator is of order λ^2 resulting in higher order diagrams to contribute at order λ^2. On general grounds we expect the contribution of higher order diagrams to merely shift the location of the poles and zeros without affecting their order such that the S-matrix takes the form

$$S(\theta) = \big(g(\theta) + O(\lambda^2)\big) \prod_i \frac{\theta - \theta_{z_i}}{\theta - \theta_{p_i}}\,, \tag{C.24}$$

where $\theta_{z/p}$ are determined up to $O(\lambda^4)$.

References

[1] R. Rattazzi, V.S. Rychkov, E. Tonni and A. Vichi, *Bounding scalar operator dimensions in 4D CFT*, *JHEP* **12** (2008) 031 [arXiv:0807.0004] [INSPIRE].

[2] V.S. Rychkov and A. Vichi, *Universal Constraints on Conformal Operator Dimensions*, *Phys. Rev.* **D 80** (2009) 045006 [arXiv:0905.2211] [INSPIRE].

[3] F. Caracciolo and V.S. Rychkov, *Rigorous Limits on the Interaction Strength in Quantum Field Theory*, *Phys. Rev.* **D 81** (2010) 085037 [arXiv:0912.2726] [INSPIRE].

[4] S. El-Showk, M.F. Paulos, D. Poland, S. Rychkov, D. Simmons-Duffin and A. Vichi, *Solving the 3D Ising Model with the Conformal Bootstrap*, *Phys. Rev.* **D 86** (2012) 025022 [arXiv:1203.6064] [INSPIRE].

[5] F. Kos, D. Poland and D. Simmons-Duffin, *Bootstrapping Mixed Correlators in the 3D Ising Model*, *JHEP* **11** (2014) 109 [arXiv:1406.4858] [INSPIRE].

[6] S. Ferrara, A.F. Grillo and R. Gatto, *Tensor representations of conformal algebra and conformally covariant operator product expansion*, *Annals Phys.* **76** (1973) 161 [INSPIRE].

[7] A.M. Polyakov, *Nonhamiltonian approach to conformal quantum field theory*, *Zh. Eksp. Teor. Fiz.* **66** (1974) 23 [INSPIRE].

[8] M.F. Paulos, J. Penedones, J. Toledo, B.C. van Rees and P. Vieira, *The S-matrix bootstrap. Part I: QFT in AdS*, *JHEP* **11** (2017) 133 [arXiv:1607.06109] [INSPIRE].

[9] M.F. Paulos, J. Penedones, J. Toledo, B.C. van Rees and P. Vieira, *The S-matrix bootstrap II: two dimensional amplitudes*, *JHEP* **11** (2017) 143 [arXiv:1607.06110] [INSPIRE].

[10] M.F. Paulos, J. Penedones, J. Toledo, B.C. van Rees and P. Vieira, *The S-matrix Bootstrap III: Higher Dimensional Amplitudes*, arXiv:1708.06765 [INSPIRE].

JHEP09(2018)052

[11] D. Mazac and M.F. Paulos, *The Analytic Functional Bootstrap I: 1D CFTs and 2D S-Matrices*, arXiv:1803.10233 [INSPIRE].

[12] S. Weinberg, *Reminiscences of the Standard Model*, lecture at ICTP, Trieste, Italy, 17 October 2017, https://www.youtube.com/watch?v=mX2R8-nJhLQ, min. 27–30 and min. 73.

[13] R.J. Eden, P.V. Landshoff, D.I. Olive and J.C. Polkinghorne, *The analytic S-matrix*, Cambridge University Press, Cambridge U.K. (1966) [INSPIRE].

[14] J.L. Miramontes, *Hermitian analyticity versus real analyticity in two-dimensional factorized S-matrix theories*, *Phys. Lett.* **B 455** (1999) 231 [hep-th/9901145] [INSPIRE].

[15] A.B. Zamolodchikov, *Exact S-Matrix of Quantum sine-Gordon Solitons*, *JETP Lett.* **25** (1977) 468 [INSPIRE].

[16] I. Arefeva and V. Korepin, *Scattering in two-dimensional model with Lagrangian* $L = (1/\gamma)[(1/2)(\partial_\mu u)^2 + m^2(\cos u - 1)]$, *Pisma Zh. Eksp. Teor. Fiz.* **20** (1974) 680 [INSPIRE].

[17] L.D. Landau and E.M. Lifshits, *Course of Theoretical Physics. Volume 3: Quantum Mechanics: Non-Relativistic Theory*, Butterworth-Heinemann, Oxford U.K. (1991) [INSPIRE].

[18] G. Mussardo and P. Simon, *Bosonic type S-matrix, vacuum instability and CDD ambiguities*, *Nucl. Phys.* **B 578** (2000) 527 [hep-th/9903072] [INSPIRE].

[19] F.A. Smirnov and A.B. Zamolodchikov, *On space of integrable quantum field theories*, *Nucl. Phys.* **B 915** (2017) 363 [arXiv:1608.05499] [INSPIRE].

[20] M. Lüscher and U. Wolff, *How to Calculate the Elastic Scattering Matrix in Two-dimensional Quantum Field Theories by Numerical Simulation*, *Nucl. Phys.* **B 339** (1990) 222 [INSPIRE].

[21] M. Creutz, *Rigorous bounds on coupling constants in two-dimensional field theories*, *Phys. Rev.* **D 6** (1972) 2763 [INSPIRE].

[22] S. Dubovsky, R. Flauger and V. Gorbenko, *Solving the Simplest Theory of Quantum Gravity*, *JHEP* **09** (2012) 133 [arXiv:1205.6805] [INSPIRE].

[23] A.B. Zamolodchikov, *Z_4-symmetric factorized S-Matrix in two space-time dimensions*, *Commun. Math. Phys.* **69** (1979) 165 [INSPIRE].

[24] G. Mussardo and S. Penati, *A Quantum field theory with infinite resonance states*, *Nucl. Phys.* **B 567** (2000) 454 [hep-th/9907039] [INSPIRE].

[25] A. Cavaglià, S. Negro, I.M. Szécsényi and R. Tateo, *$T\bar{T}$-deformed 2D Quantum Field Theories*, *JHEP* **10** (2016) 112 [arXiv:1608.05534] [INSPIRE].

[26] S. Dubovsky, R. Flauger and V. Gorbenko, *Flux Tube Spectra from Approximate Integrability at Low Energies*, *J. Exp. Theor. Phys.* **120** (2015) 399 [arXiv:1404.0037] [INSPIRE].

[27] J.L. Miramontes and C.R. Fernandez-Pousa, *Integrable quantum field theories with unstable particles*, *Phys. Lett.* **B 472** (2000) 392 [hep-th/9910218] [INSPIRE].

[28] G. Mussardo, *Statistical field theory: an introduction to exactly solved models in statistical physics*, Oxford University Press, New York NY U.S.A. (2010) [INSPIRE].

[29] E.M. Stein and R. Shakarchi, *Complex Analysis*, Cambridge University Press, Cambridge U.K. (1966) [INSPIRE].

JHEP09(2018)052